Development and Optimization of an Electric Motor for Small Aircraft by Co-Simulation of a Motor Design Software and CFD

Johann Kott[1], Daniel Grimmeisen[2]

[1]Maccon GmbH, München; j.kott@maccon.de
[1]CASCATE GmbH, Stuttgart; daniel.grimmeisen@cascate.de

Summary:
The design and development process of electric motors includes several physical disciplines. Besides electromagnetics, also thermal and mechanical (noise, vibration, strength) aspects need to be analysed. Thus, the design of electric motors for high performance applications is a multiphysics problem. To achieve a high torque to mass ratio, precise knowledge of the interaction between electromagnetic losses and the thermal behaviour of an electric motor is necessary. This knowledge can be acquired using simulation. Performing magneto-thermal multiphysics simulation accounts for the interdependence between electromagnetic and thermal behaviour. One application of electric motors are e-aircrafts. Due to strict mass budgets no dedicated liquid cooling system can be installed. Instead, the air flow during flight is the only cooling method available. Prediction of natural and forced convection on the outer surface of the electric motor is challenging, since they depend on aircraft speed, air pressure and ambient temperature. This article describes the design of an electric motor for an e-aircraft in the context of air cooling. The electromagnetic aspects will be analysed using a combination of analytical and finite element methods. The thermal and aerodynamic aspects will be covered by computational fluid dynamics to analyse the complex air flow over the motor housing during different flight phases. The co-simulation software tools are setup to exchange results and to iteratively determine stable and efficient operating points.

Keywords:

SPEED, STAR-CCM+, co-simulation, multiphysics, cooling, electric motor, aircraft

1   Electric Motor for E-Aircraft

This paper deals with the electromagnetic and thermal simulation of an electric auxiliary drive for a sailplane. Aim of the auxiliary drive is to run a self-supporting take-off, to enlarge the range of the sailplane and to support a constant horizontal flight in case of bad thermal lift. Figure 1.1 shows the principle structure of the auxiliary drive:
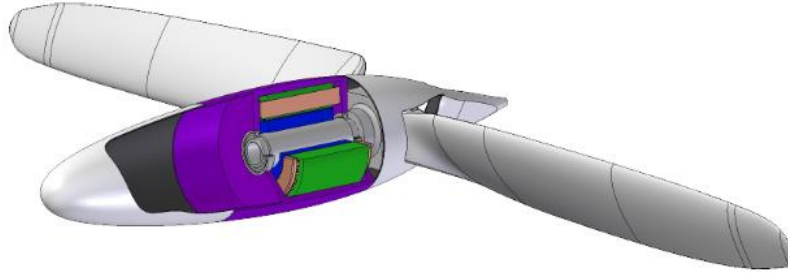
Figure 1.1 principle structure of auxiliary drive

The boundary conditions with respect to dimensions and performance were given by the sailplane manufacturer as follows:

Max. Outer Diameter [mm]	150,0
Max. Motor Length [mm]	50,0
Max. Total Mass [kg]	4,0
DC Supply voltage [V]	210,0

Figure 1.2 Mechanical requirements

	Duration [min]	Torque [Nm]	Speed [rpm]	Altitude [m]	Ambient Temperature [°C]	air flow velocity [m/s]	ambient pressure [hPa]	air density [kg/m^3]
Take-off and climb	30	33	3936	3000	18,5	35	721	0,86
Horizontal flight	continous	16,9	2826	3000	18,5	35	721	0,86

Figure 1.3 Performance requirements

The main challenge is to design a customized electric motor that fulfils the performance requirements while taking into account the load duty cycle and the cooling by the air flow. On the base of the tables above the electromagnetic design of the motor has been developed in the CAE software Simcenter SPEED while the thermal design was done in Simcenter STAR-CCM+.

2   Electromagnetic Design in Simcenter SPEED

Simcenter SPEED is a motor design software that is able to run electromagnetic simulations based on analytic equations as well as on finite element method. Mostly the finite element solver is used to calibrate the analytic formulations in order to combine the computation speed of analytics with the accuracy of FEM.
The motor design that has been developed for the sailplane auxiliary drive is a compromise between torque density, mass and mechanical stiffness. For the rotor an interior permanent magnet design has been chosen.
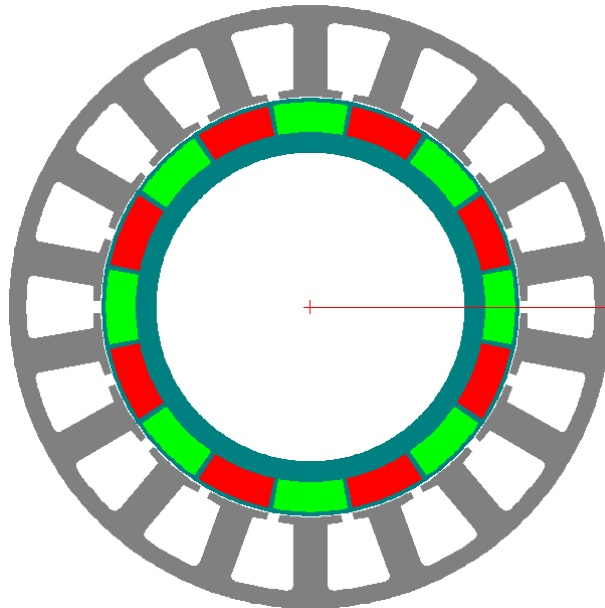
Figure 2.1 2D representation of motor design

According to the performance requirements there is no broad speed range required. For a high torque density and a narrow speed range often a surface permanent magnet rotor is the best solution. But at high speed the radial forces on the magnets have to be taken into account. It can be seen in Figure 2.1 that the chosen rotor topology is highly similar to a surface permanent magnet design, except that the magnets have been embedded in the rotor in order to protect them against radial forces.

For the stator a single tooth winding design has been used. This type of winding design ensures short end windings which gives the possibility to enlarge the active length of the motor. In order to achieve a maximum of torque in given overall dimensions it is necessary to take advantage of the maximum possible active motor length. If the axial dimension is fixed, then the active lamination length can only be increased by decreasing the end winding length. The developed motor design has the following global mechanical data.

Stator Outer Diameter [mm]	146,0
Rotor Inner Diameter [mm]	75,0
Lamination Active Length [mm]	50,0
Total Motor Length [mm]	79,5
Total Motor Mass (excl. Cables) [kg]	3,6

Figure 2.2 Dimensions of final design

The simulation of the load points in Figure 1.3 has been performed using the analytic solver. But the analytic equations have been calibrated with the finite element method. Figure 2.2 and Figure 2.3 show the FEA based distribution of magnetic flux density, iron losses in lamination and eddy current losses in one magnet under maximum load (take-off and climb).
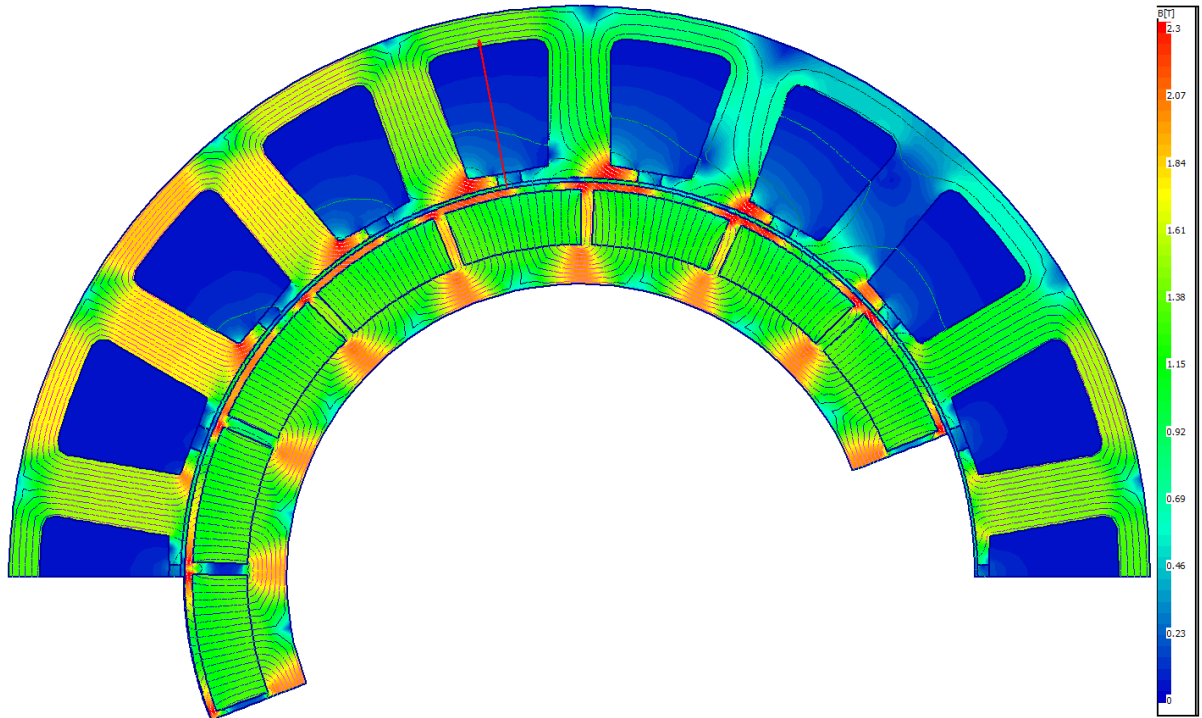
Figure 2.3 Flux density for take-off phase
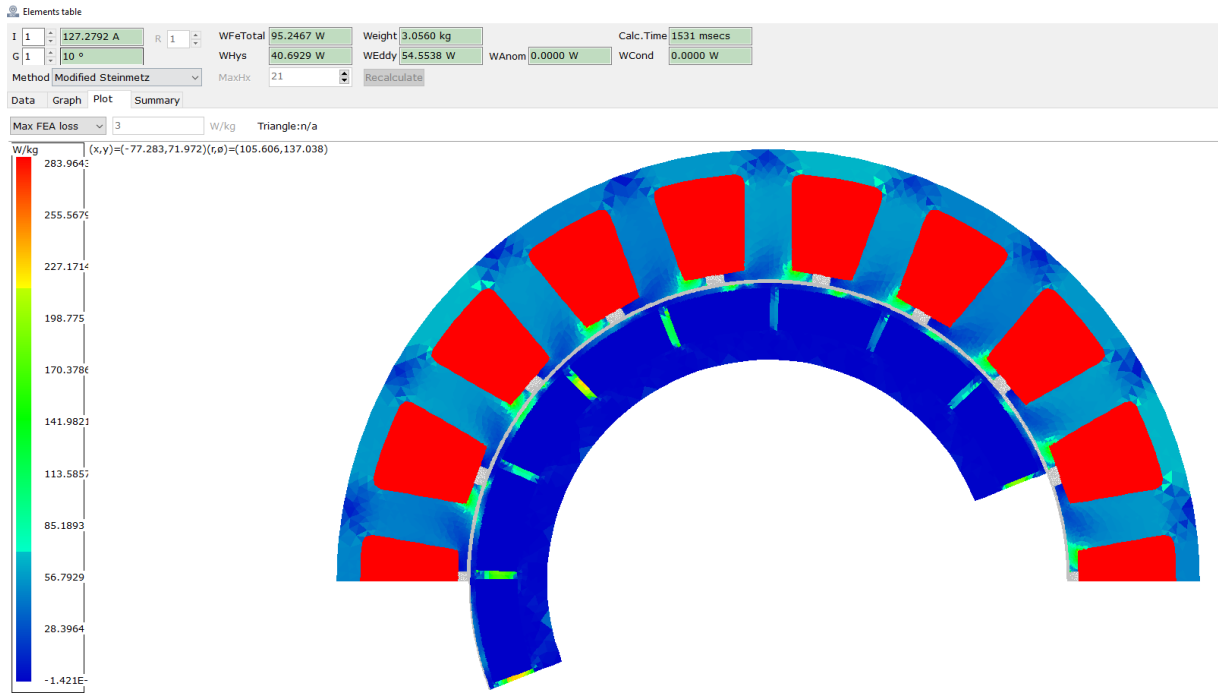
Figure 2.4 Iron and copper losses
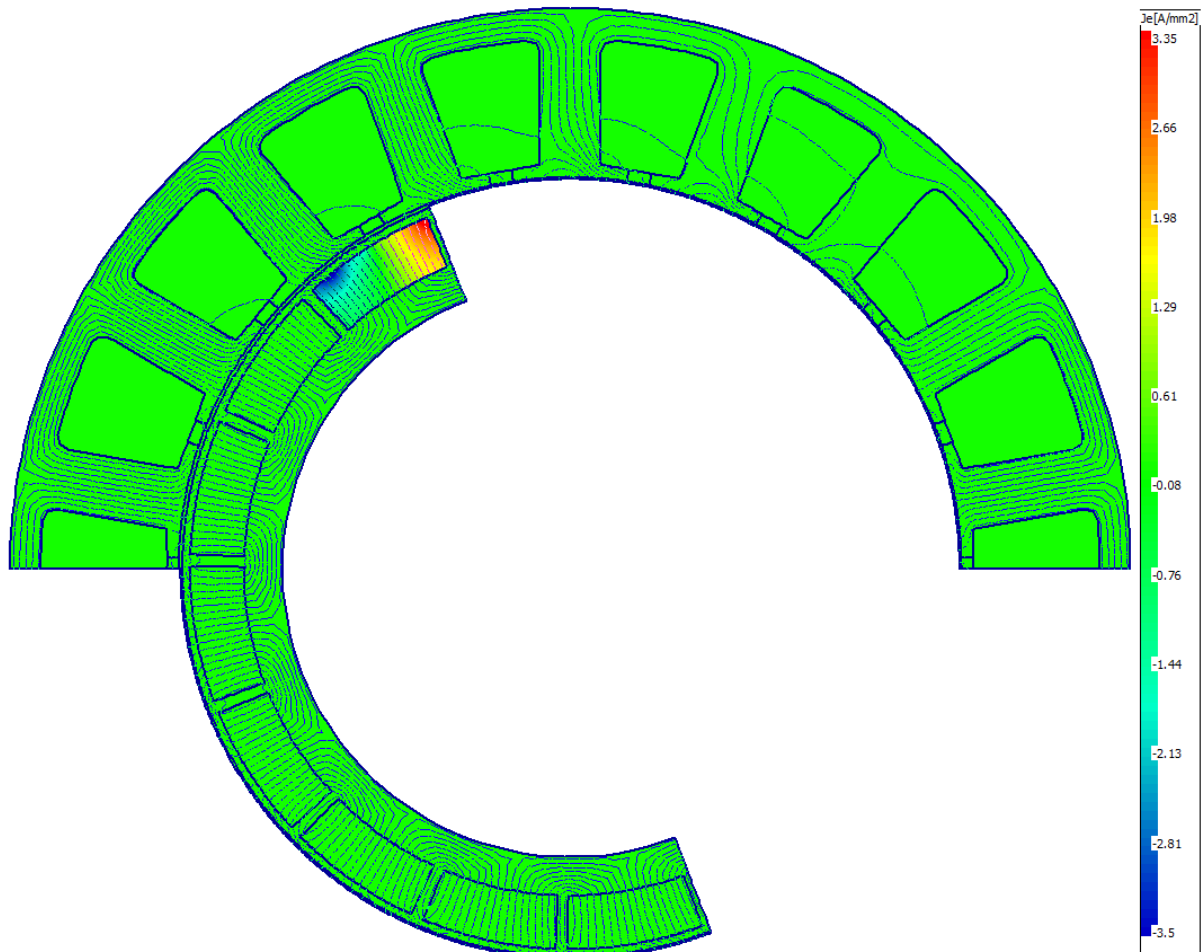
Figure 2.5 induced eddy current in one magnet

The analytic circuit equations have been calibrated using FEA based magnetic flux density and iron losses. The following tables show the analytic simulation without and with FEA calibration. The magnet losses are low compared to iron and copper losses and also a segmentation of the magnets for further loss reduction was planned. Therefore, the magnet losses have been neglected for all further simulations.

	Torque [Nm]	Speed [rpm]	Copper Losses [W]	Iron Losses [W]	Magnet Losses [W]	Efficien [%]
Take-off and climb	33,0	3936,0	436,0	97,0	0,0	96,8
Horizontal flight	16,9	2826,0	116,0	65,0	0,0	97,0

Figure 2.6 Simulation results without FEA calibration

	Torque [Nm]	Speed [rpm]	Copper Losses [W]	Iron Losses [W]	Magnet Losses [W]	Efficien [%]
Take-off and climb	33,0	3936,0	508,0	95,0	1,2	96,4
Horizontal flight	16,9	2826,0	106,0	58,0	1,2	97,2

Figure 2.7 Simulation results with FEA calibration

The results in the tables above have been calculated for fixed winding and magnet temperature. But the motor will heat up due to copper and iron losses. This leads to a higher winding resistance and a lower remanence flux density in the magnets. To compensate the lower magnet remanence a higher current is required to produce the same amount of torque. Both, higher current and higher winding resistance lead to higher copper losses which causes further temperature rise. In fact, this is an iterative process where the motor temperature rises until it reaches a steady state. In order to calculate the thermal behaviour of the motor the CFD software STAR-CCM+ was used. Fig. 2.5 shows the iterative loop between electromagnetic and thermal simulation. This loop runs until a steady state has been reached.
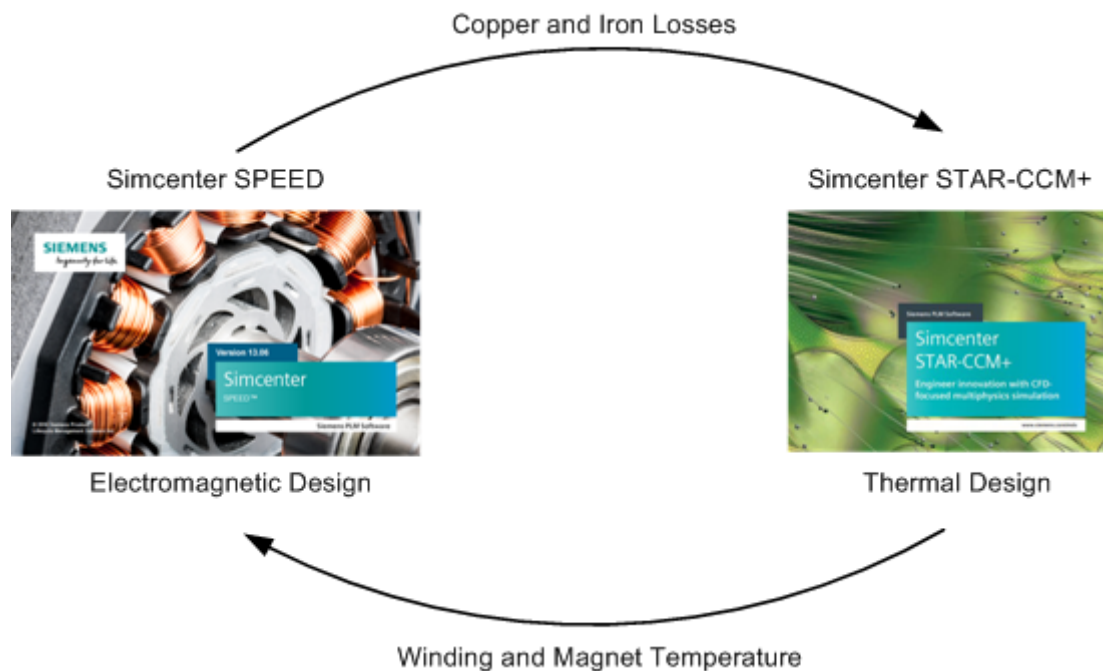
Figure 2.8 Simulation loop

3 Thermal Design in STAR-CCM+

This chapter describes the configuration as it is setup in STAR-CCM+.

3.1 Geometry

The geometry of the motor is imported into STAR-CCM+ using the *.xGDF file format. The file is generated by SPEED. Whereas SPEED is a 2D tool, geometry information is given in 3D. Additionally, a hull geometry is imported to account for an aerodynamically advantageous housing that surrounds the motor. The motor is attached within this nacelle by a bearing that also ensures conductive heat transfer. Several simplifications were carried out to optimize simulation performance. The propeller was not used in this test case since it has small effect on heat transfer. Also, the shaft that would connect motor and propeller was shortened to only span the width of the motor. Around the nacelle, the stream of air is modeled in a cylindrical area. The model is shown in Figure 3.1.
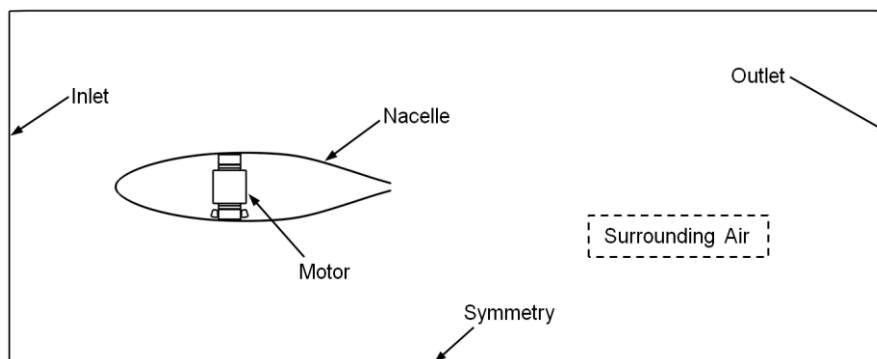
Figure 3.1 Computational Domain

3.2 Computational Mesh

One computational mesh is generated within STAR-CCM+. The interfaces between parts are non-conformal to allow for different sizes of the surface meshes on part boundaries. Mostly, polyhedral cells are used. In the fluid area, five prismatic layers are generated near the walls to resolute the boundary layer. The thin hull is discretized by four layers of prismatic cells. The domain is bounded by an inlet, where the velocity is given as boundary condition, and an outlet, where the pressure is given. On the sides, symmetry is assumed. This is depicted in Figure 3.1. The volumetric fluid mesh is refined in vicinity to the areas of higher curvature at the leading and trailing edge of the nacelle as well as near the motor.

Altogether, the mesh consists of 230'000 cells in the fluid area, 250'000 cells in the hull and 88'000 cells in the motor.

3.3 Physics Modeling

To assess the thermal efficiency of cooling, steady-state RANS simulations are carried out. As an indicator for convergence, relative change of the temperature within the motor is monitored. Gravity is factored in since it drives natural convection of the air close to the motor. To account for turbulence, the realizable k-epsilon turbulence model is used. The flow field consists of both areas with high Reynolds numbers in the free stream as well as areas with low Reynolds numbers within the nacelle. Thus, the two-layer approach is used where the region is divided up into two layers. In the layer close to the walls, turbulent dissipation rate and turbulent viscosity are calculated as functions of the wall distance [1]. The energy equation is solved in the flow field since heat is transferred through natural and forced convection. The density is assumed to be constant and given through external calculation depending on the regarded flight altitude. The SIMPLE algorithm is used to couple pressure and velocity [2].

Various solid regions exist for the different materials of motor and hull. Material properties of the motor are as specified in SPEED, the material of the hull is aluminum. In all solid regions the energy equation is solved to determine heat distributions.

3.4 Linking SPEED and STAR-CCM+

Temperatures in the motor influence the characteristics of the motor performance. Also, cooling influences the motor temperatures. As such, both thermal as well as electromagnetic simulation influence one another and have to be intertwined. Two motor characteristics are streamed from SPEED to STAR-CCM+, that being heat loss in the stator and in the windings. These heat losses are incorporated as heat sources on the surfaces of said regions in STAR-CCM+. The ensuing magnet and windings maximum temperatures are reported back to SPEED as initial conditions for the next iteration.

4 Results

To obtain results, two criteria are setup to determine convergence. Within STAR-CCM+, the steady-state simulation is considered converged when the maximum temperature in the windings changes less then by a defined threshold over ten iterations. Likewise, the feedback loop between SPEED and STAR-CCM+ is considered complete once the same temperature changes by less than a defined threshold between two iterations.

	PFes [W]	WCu [W]	T_mag [K]	T_Wdg [K]
i0	15.821964	507.54612	373.0247	380.304
i1	7.437204	681.791643	397.9827	408.0805
i2	5.437956	737.229001	406.0058	417.0246
i3	4.858318	755.079964	408.6035	419.133
i4	4.677236	759.287986	409.1917	420.5858
i5	4.636682	762.187538	409.6568	421.0704
i6	4.604733	763.15472	409.7773	421.2284
i7	4.596472	763.470062	409.811	421.2767
i8	4.594363	763.566461	409.8343	421.2989
i9	4.592567	763.610769	409.8529	421.3094

Figure 4.1 Looped Parameters for the take-off and climb case

	PFes [W]	WCu [W]	T_mag [K]	T_Wdg [K]
i0	8.940921	105.345114	310.3948	311.5712
i1	7.80158	113.02384	311.421	312.6835
i2	7.736138	113.484552	311.4875	312.7528
i3	7.731907	113.513256	311.4913	312.7571
i4	7.731665	113.515037	311.4983	312.7628

Figure 4.2 Looped parameters for the horizontal flight case

Figures 4.1 and 4.2 show the parameters that are exchanged between the two tools during each iteration i. PFes is the iron loss, WCu is the copper loss, both determined by SPEED. T_mag is the temperature in the magnet, T_Wdg is the temperature in the windings, both determined by STAR-CCM+. With each additional iteration step, the temperatures and losses approach an asymptotic value. The take-off and climb case takes more steps to converge since temperatures and losses are at a generally higher level. The horizontal case converges quickly. As expected, temperatures are highest during take-off and climb. Figure 4.3 shows the heat distribution on the hull for the last iteration step of the horizontal flight case.
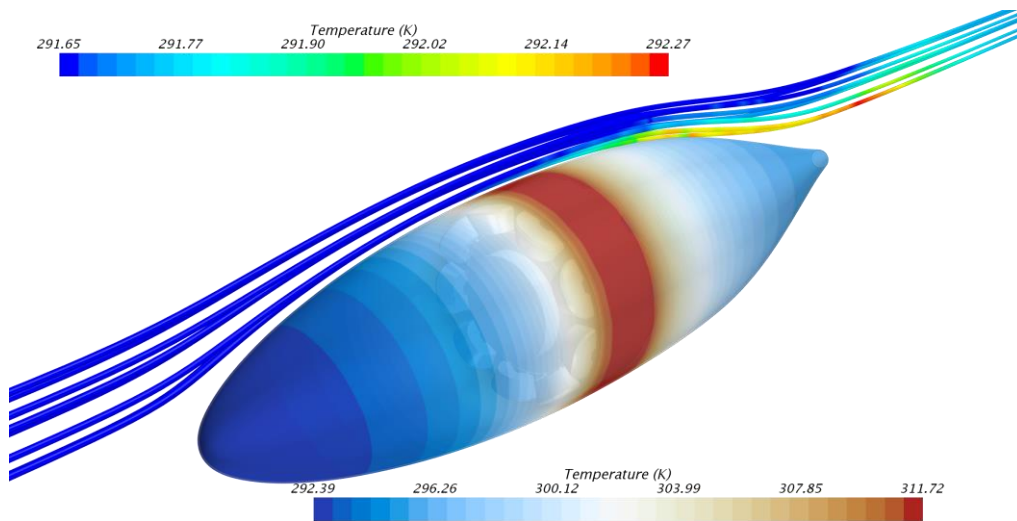
Figure 4.3 Temperature distribution on the nacelle for the horizontal flight test case

The hull heats up most in close vicinity to the motor. Air that flows around the hull heats up as well once it passes the high temperature areas on the hull surface. The two governing heat transfer mechanisms are convection and conduction. Air surrounding the motor heats up, rises and meets the inner wall of the hull, to which it then transfers heat. This is visualized in Figure 4.4.
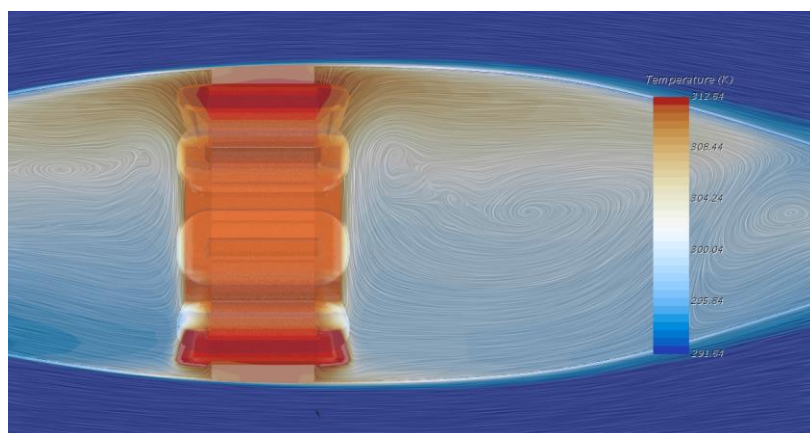
Figure 4.4 Streamlined vector field within the nacelle

This figure shows the streamlines that are integrated using the vector field of the flow within the nacelle. Air rises near the motor and falls away from the motor. This leads to an overlaying vortex within the nacelle. It has to be noted that in the real geometry, the interior space within the nacelle is not empty. Thus, air cannot flow as freely.

The simulations in SPEED yield results almost immediately. The simulations in STAR-CCM+ take between two minutes for the last loops per test case and one hour for the first loops per test case to finish on a six core workstation. Together, the horizontal test case took approximately 90 minutes to finish and the take-off and climb test case took approximately four hours to finish.

5   Conclusion

It was shown that SPEED and STAR-CCM+ can be setup to co-simulate the electro-thermal behavior of an e-motor. For two test cases, heat losses of copper and iron were calculated in SPEED. They were then mapped onto the stator and windings surfaces in STAR-CCM+ as heat sources. In the cooling simulation, the resulting heat was carried off into the hull by convection through air and by conduction through a bearing. Within the hull, the heat was distributed to the outer surface where it transferred to the external flow. Thus, a steady state with fixed temperatures in all regions could be achieved. The temperatures in the windings and in the magnets lead to a changed performance of the motor and were therefore fed back into SPEED to close the loop. That way, simulation can hint on whether cooling performance is sufficient for an electric motor without having to use costly experiments.

6   References

[1]   Rodi, W. 1991. "Experience with Two-Layer Models Combining the k-e Model with a One-Equation Model Near the Wall", 29th Aerospace Sciences Meeting, January 7-10, Reno, NV, AIAA 91-0216

[2]   Siemens PLM Software: Documentation of STAR-CCM+ v2019.2